Spin dynamics and thermodynamics in solid-state NMR cross polarization

M. H. Levitt,[a] D. Suter, and R. R. Ernst
Laboratorium für Physikalische Chemie, Eidgenössische Technische Hochschule, 8092 Zürich, Switzerland

(Received 24 October 1985; accepted 10 January 1986)

We investigate spin thermodynamic processes taking place during Hartmann–Hahn cross-polarization experiments in solids, in which spin polarization is transferred between two nuclear spin species by the application of two strong rf fields. As is well known, optimum cross polarization is achieved for a particular ratio of the two rf field strengths called the Hartmann–Hahn condition; we find experimentally that this condition provides the optimum transfer not only on kinetic grounds, as is usually supposed, but also for thermodynamic reasons. By measurement of the evolution of the spin observables in a ferrocene single crystal we demonstrate the existence of a quasi-equilibrium state with nonuniform spin temperature and less than maximum entropy. A modified spin thermodynamic theory is developed whose main features are the important role of the dipolar energy for the quasi-equilibrium state and the existence of constants of the motion other than the total energy. A new cross-polarization experiment is suggested which is shown to provide efficient cross polarization even for mismatched Hartmann–Hahn conditions.

I. INTRODUCTION

Cross polarization in the rotating frame[1–15] is the most widely used technique today for enhancing the nuclear spin polarization of isotopes of low gyromagnetic ratio, such as ^{13}C and ^{15}N, in solids. Especially in conjunction with heteronuclear decoupling and magic-angle spinning,[8,9] cross-polarization techniques for transferring the comparatively large and rapidly established spin polarization of species such as protons to rare nuclei of low gyromagnetic ratio have made possible truly routine high-resolution solid-state NMR.[6,7] Cross polarization has also been applied for enhancing multiple quantum transitions,[10–13] for sensitivity enhancement in high-resolution NMR of isotropic liquids,[14,15] and for the indirect detection of resonance.[2–4]

There are two common experimental schemes for cross polarization between spin species I and S, involving either adiabatic demagnetization in the rotating frame (ADRF) of the abundant spin reservoir,[3] or simultaneous spin locking of the two species as first proposed by Hartmann and Hahn.[1] The latter is experimentally simpler, and is indeed the only practical method for a rotating sample. Nevertheless the ADRF case has been the subject of the most detailed experimental study to date. The dependence of the cross polarization rate on the strength of the rf field applied to the S spins was the object of interest and could be explained with remarkable accuracy.[3,16]

By comparison with this close scrutiny of the ADRF method of cross polarization, few investigations of the processes occuring during Hartmann–Hahn cross polarization have been made. The most common theoretical description of Hartmann–Hahn cross polarization, which is found in many publications and textbooks,[5–7] is in serious discrepancy with experimental observations. This theory describes the system by separate I and S spin reservoirs, which are free to exchange energy in arbitrarily small units, and predicts that on attainment of quasi-equilibrium the cross-polarized S spin polarization increases in proportion with the heat capacity of the S spin reservoir and therefore with the strength of the rf field applied to the S spins. However, the experimental observation is almost always that optimum cross polarization is achieved for equal nutation frequencies about the rf fields applied to the two spin species (Hartmann–Hahn match). Further increase of the S spin rf field beyond this value usually reduces the amount of cross-polarized magnetization. This discrepancy is normally explained by assuming that the rate of cross polarization decreases rapidly away from match, so that in fact quasi-equilibrium is not attained except when the rf nutation frequencies are equal.[5–7] Again this is unsupported by experiment: In practice, we find that away from Hartmann–Hahn match, the S spin polarization grows initially at a rate which is not much different from that under matched conditions, but levels off earlier. The system appears to reach a quasi-equilibrium which under mismatched conditions is less favorable with respect to creation of S polarization than under matched conditions. [An example is shown in Fig. 5(c).] The "usual" theory provides no explanation of this unfavorable quasi-equilibrium. However, Demco *et al.*[16] could predict such behavior by detailed dynamical calculations using a memory function approach, as is shown in their Fig. 9.[16] It is our intention in this article to examine the nature of the quasi-equilibrium and to explain at least qualitatively its properties.

It is shown that it is necessary to include the thermodynamic effects of dipolar couplings in order to explain the observed behavior. As has been pointed out by several workers,[17–26] dipolar couplings have in many situations a significant influence on spin thermodynamics even though they may be much weaker than the Zeeman interactions. This arises because they are directly involved in absorbing energy mismatches.

Previous studies of cross polarization[3,16] were often performed on single crystals of calcium fluoride CaF_2, where

[a] Present address: Francis Bitter National Magnet Laboratory, MIT Building NW14-5122, Cambridge, Massachusetts 02139.

 0021-9606/86/084243-13$02.10 © 1986 American Institute of Physics

cubic symmetry makes the calculation of lattice sums relatively easy. We chose instead a system for experimental study which, although more complicated, resembles more closely the practically important case of natural abundance ^1H–^{13}C cross polarization in organic solids, namely a single crystal of ferrocene [$Fe(C_5H_5)_2$], doped with ~2% cobaltocene in order to reduce the ^1H spin-lattice relaxation time to about 1 s. In ferrocene, internal rotations about the C_5 symmetry axis reduce the magnitude of the dipole couplings. In most orientations of the crystal with respect to the static magnetic field, the heteronuclear ^{13}C–^1H coupling between directly bonded atoms exceeds all other couplings. A major consequence of the dominance of a single coupling is a transient oscillatory dependence of the cross-polarized magnetization on the cross-polarization time.[27] These transient oscillations, in combination with two-dimensional (2D) spectroscopy[28] have been used to measure heteronuclear dipole couplings in organic solids.[24–31] The full time dependence during cross polarization under Hartmann–Hahn matched conditions has previously been explained in a qualitative manner for ferrocene assuming that the system may be treated as an ensemble of spin pairs (^{13}C spins and their directly bonded protons) in thermal contact with a reservoir made up of the other protons.[27] We will extend this model and attempt also to explain the quasi-equilibrium existing under Hartmann–Hahn mismatched conditions. As will be shown theoretically and experimentally, mismatched Hartmann–Hahn cross polarization creates a substantial amount of heteronuclear dipolar order.

We show that understanding the nature of the quasi-equilibrium allows the design of a cross-polarization method which provides successful transfer of magnetization to the ^{13}C spins even under grossly mismatched Hartmann–Hahn conditions. This new technique resembles the conventional spin-lock cross polarization but involves repeated π phase shifts on both irradiation channels simultaneously. Under Hartmann–Hahn mismatched conditions, the simultaneous phase shifts invert the temperature of the dipolar bath with respect to the I and S spin bath. The system then evolves towards a new quasi-equilibrium which is often more favorable with respect to S spin polarization. The new method may be useful for cross polarization in static solids where resolved heteronuclear couplings exist.

The organization of the rest of this paper is as follows: In Sec. II a short description of the cross-polarization experiment is given, and the various spin thermodynamic treatments are contrasted. Intenal thermal equilibrium processes, quasi-equilibrium, and complete thermal equilibrium are described as successive projections of the density operator onto subspaces of decreasing number of dimensions. A description of cross polarization taking into account the effect of the dipolar couplings is given in these terms. Section III concerns cross polarization in the presence of resolved heteronuclear couplings and contains the principal experimental results obtained for ferrocene. Modifications to the projection operator theory for resolved heteronuclear couplings are suggested. Experimental results and theory for the mismatch-optimized $I \rightarrow S$ transfer experiment (abbreviated MOIST) which in suitable cases provides effective transfer even for mismatched Hartmann–Hahn conditions, are given. Section IV concerns some special procedures necessary to obtain accurate measurements of spin observables like S spin polarization and heteronuclear dipolar order.

II. THEORIES OF CROSS POLARIZATION

A. The cross-polarization experiment

Cross polarization in the rotating frame was introduced by Hartmann and Hahn.[1] A system of two nuclear spins, I and S, is simultaneously irradiated with two rf fields B_{1I} and B_{1S} of frequencies ω_I and ω_S close to the Larmor frequencies ω_{0I} and ω_{0S}. If the resonant offsets are small, and the nutation frequencies ω_{1I} and ω_{1S} around the two fields are such that the Hartmann–Hahn condition is satisfied:

$$|\omega_{1I}| = |\omega_{1S}|, \tag{1}$$

where

$$\omega_{1I} = -\gamma_I B_{1I}, \quad \omega_{1S} = -\gamma_S B_{1S},$$

then thermodynamic contact between the two nuclear spin species is achieved. By convention we assume that each field is applied along the x axis in its respective rotating frame. A usual experiment involves first creating a large polarization of the abundant spins I along the rotating frame field by thermal equilibration in the large static magnetic field B_0, followed by a $(\pi/2)_y$ pulse. Under Hartmann–Hahn contact the polarization $\langle I_x \rangle$ of the abundant spins is partially transferred to polarization $\langle S_x \rangle$ of the rare spins. After completion of the observation of the S spin signal an additional $(\pi/2)_{-y}$ pulse on the I spins "flips back" their magnetization to the axis parallel with B_0, preventing its destruction during the relaxation period between experiments and allowing a faster repetition rate[32] (Fig. 1).

B. The system

We consider a static solid containing two nuclear spin species, I and S. The I spins are assumed to be abundant and the S spins rare, so that S–S interactions may be ignored, and it is valid to treat the system as an ensemble of subsystems, each consisting of a single S spin and a large number of I spins. In the "doubly rotating" interaction frame,[7] the Hamiltonian is given after the usual high-field truncations by

$$\mathcal{H} = \mathcal{H}_I + \mathcal{H}_S + \mathcal{H}_{IS} + \mathcal{H}_{II},$$

where

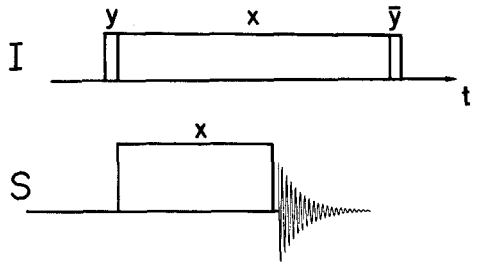

FIG. 1. Conventional double resonance irradiation scheme for Hartmann–Hahn cross polarization in order to transfer I spin Zeeman polarization to S spin polarization. The usual notation $x, y, \bar{x}, \bar{y}$ is used for the four orthogonal irradiation phases. The narrow rectangles are 90° pulses. The last 90° pulse on the I spins flips back the spin-locked magnetization along the z axis.

$$\mathcal{H}_I = \sum_k \Omega_k I_{kz} + \omega_{1I} \sum_k I_{kx},$$
$$\mathcal{H}_S = \Omega_S S_z + \omega_{1S} S_x, \tag{2}$$
$$\mathcal{H}_{IS} = \sum_k b_k 2 I_{kz} S_z,$$
$$\mathcal{H}_{II} = \sum_j \sum_k d_{jk} \left[2 I_{jz} I_{kz} - \frac{1}{2} (I_j^+ I_k^- + I_j^- I_k^+) \right],$$

where Ω_k and Ω_s are resonance offsets and ω_{1I} and ω_{1S} rf-field strengths. The heteronuclear dipolar coupling constants b_k between the S spin and the I spins I_k, and the homonuclear II dipolar coupling constants d_{jk}, are given by

$$b_k = -\frac{\mu_0 \gamma_I \gamma_S \hbar^2}{4\pi r_k^3} \frac{1}{2} (3 \cos^2 \theta_k - 1)$$

and

$$d_{jk} = -\frac{\mu_0 \gamma_I^2 \hbar^2}{4\pi r_{jk}^3} \frac{1}{2} (3 \cos^2 \theta_{jk} - 1), \tag{3}$$

where r_k, and r_{jk} are internuclear distances and θ_k, and θ_{jk} are angles between internuclear vectors and the static magnetic field. Scalar couplings have been ignored and all constants are in angular frequencies units. For simplicity we assume in the following that the offsets Ω_k and Ω_S are negligibly small and may be ignored. Generalization is not difficult.

In the case of strong irradation on both channels, $|\omega_{1I}| \gg |d_{jk}|$, $|\omega_{1S}| \gg |b_k|$, it is convenient to write the Hamiltonian in a frame rotated about the y axis defined by

$$A^T = \exp\left[i \frac{\pi}{2} \left(\sum_k I_{ky} + S_y \right) \right] \times A \exp\left[-i \frac{\pi}{2} \left(\sum_k I_{ky} + S_y \right) \right], \tag{4}$$

giving

$$\mathcal{H}^T = \mathcal{H}_I^T + \mathcal{H}_S^T + \mathcal{H}_{IS}^T + \mathcal{H}_{II}^T,$$

with

$$\mathcal{H}_I^T = \sum_k \omega_{1I} I_{kz}, \quad \mathcal{H}_S^T = \omega_{1S} S_z,$$
$$\mathcal{H}_{IS}^T = \sum_k b_k 2 I_{kx} S_x, \quad \mathcal{H}_{II}^T = \mathcal{H}_{II}^{T'} + \mathcal{H}_{II}^{T''},$$
$$\mathcal{H}_{II}^{T'} = -\frac{1}{2} \sum_{jk} d_{jk} \left[2 I_{jz} I_{kz} - \frac{1}{2} (I_j^+ I_k^- + I_j^- I_k^+) \right],$$

and

$$\mathcal{H}_{II}^{T''} = \frac{3}{2} \sum_{jk} d_{jk} \frac{1}{2} (I_j^+ I_k^+ + I_j^- I_k^-). \tag{5}$$

The homonuclear dipolar interaction Hamiltonian in the tilted frame $\mathcal{H}_{II}^T$ has been divided into terms $\mathcal{H}_{II}^{T'}$ and $\mathcal{H}_{II}^{T''}$ secular and nonsecular with respect to the large Hamiltonian $\mathcal{H}_I^T$. For large I spin fields ($|\omega_{1I}| \gg |d_{jk}|$) the nonsecular terms $\mathcal{H}_{II}^{T''}$ may usually be ignored.

We assume that the initial spin density operator σ is prepared as

$$\sigma(0) = \left\{ 1 - \frac{\hbar \omega_{0I}}{kT_L} \sum_k I_{kx} \right\} \Big/ \mathrm{Tr}\{1\}$$

by an initial $(\pi/2)_y$ pulse on the I spins applied to a system in thermal equilibrium at the high lattice temperature T_L in the static field B_0. (The initial polarization of the S spins is assumed to be small or may be removed experimentally by presaturation.) Defining $\alpha_{0I} = -\hbar\omega_{0I}/(kT_L \mathrm{Tr}\{1\})$, the initial density operator in the tilted frame is

$$\sigma^T(0) = \alpha_{0I} \sum_k I_{kz}, \tag{6}$$

neglecting the unity operator term. This evolves under the equation of motion

$$\dot{\sigma}^T = -i[\mathcal{H}^T, \sigma^T]. \tag{7}$$

The Hamiltonian of Eq. (5) is far too complicated for Eq. (7) to be integrated exactly. One often finds empirically, however, that after a sufficiently long time (which is still short compared to spin-lattice relaxation), the system attains a state of "quasi-equilibrium" in which the observables such as magnetization, dipolar order, etc., do not appear to change any more.

It is possible to analyze either the dynamical evolution of the system towards quasi-equilibrium, as done most thoroughly by Demco *et al.*[16] using many-body techniques such as memory function theory, or to investigate the nature of the quasi-equilibrium state itself, in which case spin thermodynamic methods are appropriate.[21,22] It is the latter course which is followed here.

C. Spin thermodynamic theory

1. General aspects

All theories of spin thermodynamics set out by separating the Hamiltonian of the spin system into a set of thermodynamic reservoir terms $\mathcal{H}_i^0$, and a smaller perturbation term V,

$$\mathcal{H} = \mathcal{H}^0 + V,$$
$$\mathcal{H}^0 = \sum_i \mathcal{H}_i^0,$$

where

$$[\mathcal{H}^0, V] \neq 0,$$
$$[\mathcal{H}_i^0, \mathcal{H}_j^0] = 0. \tag{8}$$

$\mathcal{H}^0$ is considered to include the principal contributions to the energy of the spin system; the energy associated with the perturbation V is ignored, it being assumed that V plays a purely kinetic role in mediating the flow of energy and spin order between the thermodynamic reservoirs $\mathcal{H}_i^0$. The reservoir terms $\mathcal{H}_i^0$ are usually arranged to be orthogonal

$$(\mathcal{H}_i^0 | \mathcal{H}_j^0) = 0, \quad i \neq j, \tag{9}$$

where $(A|B) = \mathrm{Tr}\{A^\dagger B\}$, so that the expectation values (energies) of each are independent and additive:

$$\langle \mathcal{H} \rangle \simeq \langle \mathcal{H}^0 \rangle = \sum_i \langle \mathcal{H}_i^0 \rangle. \tag{10}$$

The above decomposition can be made in a number of different ways. The proper choice is often a matter of physical intuition supported eventually by agreement of theory with experiment. However, some qualitative guidelines may be given[21]: Each term $\mathcal{H}_i^0$ should have either (a) a harmonic

spectrum (equally spaced eigenvalues), or (b) a dense spectrum with a very large number of closely spaced eigenvalues.

Typical examples of (a) and (b) are on the one hand the Zeeman Hamiltonian of a system of identical spins, and on the other hand the high-field secular dipolar Hamiltonian. The above conditions for the reservoir Hamiltonians are necessary because it will be assumed that the reservoirs assume rapid "internal thermal equilibrium," meaning that an arbitrary density operator $\sigma(0)$ evolves in a short time $\tau_{\rm int}$ to a state approaching

$$\sigma(\tau_{\rm int}) \simeq \sum_i \frac{(\sigma(0)|\mathcal{H}_i^0)}{(\mathcal{H}_i^0|\mathcal{H}_i^0)}\,\mathcal{H}_i^0. \tag{11}$$

Assumptions (a) or (b) allow rapid thermal equilibration within each reservoir to be plausible, in the first case because exchange of populations throughout the system of equally spaced energy levels can take place by energy conserving "flip–flops," and in the second case as a statistical approximation to a dynamical process which is in reality considerably more complicated. However, the selection criteria (a) and (b) above should be regarded as semiempirical rules whose strict justification is difficult.

Over a longer time scale $\tau_{\rm eq}$, the different reservoirs may come into thermal contact with each other, under the influence of V. If the system remains isolated for a sufficient time, and if the system is *ergodic*, meaning that the total energy is the only relevant constant of the motion, the end result will be uniform temperature across the whole spin system. This is equivalent to a maximization of entropy under the single constraint that the total energy $\langle\mathcal{H}\rangle \simeq \langle\mathcal{H}^0\rangle$ remains constant, and may be represented mathematically as the projection

$$\sigma(\tau_{\rm eq}) \simeq \frac{(\sigma(\tau_{\rm int})|\mathcal{H}^0)\mathcal{H}^0}{(\mathcal{H}^0|\mathcal{H}^0)} = \frac{(\sigma(0)|\mathcal{H}^0)\mathcal{H}^0}{(\mathcal{H}^0|\mathcal{H}^0)}. \tag{12}$$

Thus the evolution of the spin density operator is assumed to proceed in two stages: A short-time-scale evolution which leads to internal thermal equilibrium of each reservoir, and a long-time-scale evolution consisting of thermal equilibration between the reservoirs. These two projection processes are depicted for the case of two reservoirs $\mathcal{H}_1^0$ and $\mathcal{H}_2^0$ in Fig. 2. The initial density operator, represented as an arbitrary three-dimensional vector, is projected first onto the two-dimensional $\{\mathcal{H}_1^0, \mathcal{H}_2^0\}$ plane, and then finally onto the vector in this plane which represents the total Hamiltonian of the system. The collapse of the density operator, first from a vector in three dimensions to two, and then from two dimensions to one, represents processes of increasing entropy.

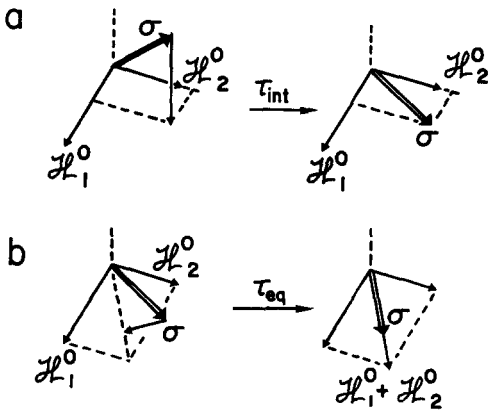

FIG. 2. Pictorial representation of ordinary spin thermodynamics in the case of two thermodynamic reservoirs, $\mathcal{H}_1^0$ and $\mathcal{H}_2^0$, represented as orthogonal vectors. (a) The initial density operator σ in general contains elements off-diagonal with respect to both $\mathcal{H}_1^0$ and $\mathcal{H}_2^0$ and must accordingly be represented as a vector of dimension greater than two; here a three-dimenisonal vector is drawn. Over a short time $\tau_{\rm int}$, thermal equilibrium is established within each of the two reservoirs and the off-diagonal parts decay to zero, which is represented pictorially as a projection of σ onto the $\{\mathcal{H}_1^0, \mathcal{H}_2^0\}$ plane. (b) Thermal contact between $\mathcal{H}_1^0$ and $\mathcal{H}_2^0$ allows establishment of a common spin temperature over a time $\tau_{\rm eq}$. This is represented as a further projection of σ onto the total Hamiltonian $\mathcal{H}^0 = \mathcal{H}_1^0 + \mathcal{H}_2^0$.

The processes discussed above differ in no way from those occuring in macroscopic "classical" thermodynamics. However, our main concern in this paper is the intermediate time-scale phenomenon of quasi-equilibrium, in which only partial thermal equilibrium between the thermodynamic reservoirs occurs, and which is a consequence of the quantization of the spin systems. It has no parallel in macroscopic thermodynamics. It is found that over a time scale $\tau_{\rm qe}$ longer than $\tau_{\rm int}$, but shorter than $\tau_{\rm eq}$, the system fails to assume the thermally fully equilibrated state Eq. (12), but instead remains in a metastable state of nonuniform spin temperature with lower entropy than in Eq. (12).

Quasi-equilibrium may be established if at least three reservoirs $\mathcal{H}_i^0$ exist, and if there are restrictions (on a realistic experimental time scale) of the possible modes of exchange of energy between them, so that the third reservoir is inevitably involved in the exchange of energy between the other two. The restrictions may ocur because of the particular structure of the energy level schemes of the reservoirs $\mathcal{H}_i^0$, or because of the form of the perturbations V which mediate the transfer of order, and have the consequence that there may be relevant quantities other than the total energy which are constants of the motion. If this *nonergodicity* is ignored, incorrect predictions are obtained. For example in many textbooks and papers,[5–7] cross polarization between I spins and S spins is described as a thermal equilibrium between the two reservoirs $\mathcal{H}_I^T$ and $\mathcal{H}_S^T$, under the influence of the IS coupling $\mathcal{H}_{IS}^T$. However, unless $|\omega_I| = |\omega_S|$ (Hartmann–Hahn condition), the spacing between the energy levels of $\mathcal{H}_I^T$ and $\mathcal{H}_S^T$ does not match, so it is obviously impossible to allow exchange of single quanta between these reservoirs whilst conserving energy. Thus this simple thermodynamic model is only usable exactly at the Hartmann–Hahn match condition and predictions made using it away from Hartmann–Hahn match are incorrect. For example the naive thermodynamic model predicts that the amount of magnetization transferred from the I spins to the S spins increases with the rf field applied to the S spins,[5,7] a prediction in conflict with experimental results which show a maximum transfer on match. The discrepancy is usually explained by invoking a rapid decrease of the cross-polarization rate away from match. However, as mentioned above, the experimental results again show this postulate to be untenable: In many cases the effect appears to be truly a thermodynamic, and not a kinetic one [see Fig. 5(c)].

The failure of the naive theory makes it clear that it is

necessary to include the effect of "broadening" the distribution of I spin energy levels by dipolar interactions so as to produce a finite width of the Hartmann–Hahn match and to allow exchange of quanta between the reservoirs while conserving energy. However, caution is again necessary; the tempting solution of replacing the reservoir $\mathcal{H}_I^T$ by the modification $\mathcal{H}_I^T + \mathcal{H}_{II}^T$ is again incorrect, since the energy level structure of the latter fulfills neither condition (a) nor (b) above; it is well known that a combined Zeeman-dipolar reservoir does not attain internal thermal equilibrium rapidly if the applied rf fields are strong. The question arises how to take into account the thermodynamic effect of quantization of $\mathcal{H}_I^T$ and $\mathcal{H}_S^T$ and the involvement of dipolar interactions. An appropriate framework for solving such problems has been given by Jeener,[21] in terms of orthogonal quasi-invariant operators. Goldman[22] has also given a treatment of cross relaxation based on similar principles which can easily be adapted for cross polarization.

The solution is based on the identification of quasi-invariants of the system, operators whose expectation values may be assumed to be conserved during the process of thermal equilibration. Suppose such a set of operators Q_q can be found, such that Q_q are orthogonal,

$$(Q_q|Q_{q'}) = 0; \quad q \neq q'.$$

It is furthermore demanded that each Q_q may be expressed as a linear combination of the terms $\mathcal{H}_i^0$, and that the operators are normalized such that

$$(\mathcal{H}^0|Q_q) = (Q_q|Q_q). \tag{13a}$$

With this normalization,

$$\mathcal{H}^0 = \sum_q Q_q, \tag{13b}$$

and it is possible to interpret the terms Q_q as new thermodynamic reservoirs, which may be operative on a time scale different to that of the previous reservoir terms $\mathcal{H}_i^0$ (see below).

The quasi-equilibrium position can be deduced by projecting the density operator $\sigma(\tau_{\text{int}})$ separately onto each quasi-invariant operator:

$$\sigma(\tau_{\text{qe}}) \simeq \sum_q \frac{(\sigma(\tau_{\text{int}})|Q_q)Q_q}{(Q_q|Q_q)}, \tag{14}$$

where τ_{qe} is a time for establishment of quasi-equilibrium, $\tau_{\text{int}} \ll \tau_{\text{qe}} \ll \tau_{\text{eq}}$. Equation (14) represents a maximization of entropy under the set of constraints that all $\langle Q_q \rangle$ remain constant: It clearly is a state of lower entropy than the fully equilibrated density operator $\sigma(\tau_{\text{eq}})$.

The evolution of the density operator from the state of internal thermal equilibrium within the resorvoirs $\mathcal{H}_i^0$ [Eq. (11)], to the state of quasi-equilibrium [Eq. (14)] may be viewed from two complementary viewpoints. On the one hand it may be regarded as a partial thermal equilibration between the reservoirs $\mathcal{H}_i^0$, which cannot proceed to completion because of the constraint that the invariants $\langle Q_q \rangle$ are conserved; on the other hand it is simply a process of thermal equilibration within each quasi-invariant term Q_q. The two points of view are complementary, and which is more useful depends on the time scale of interest.

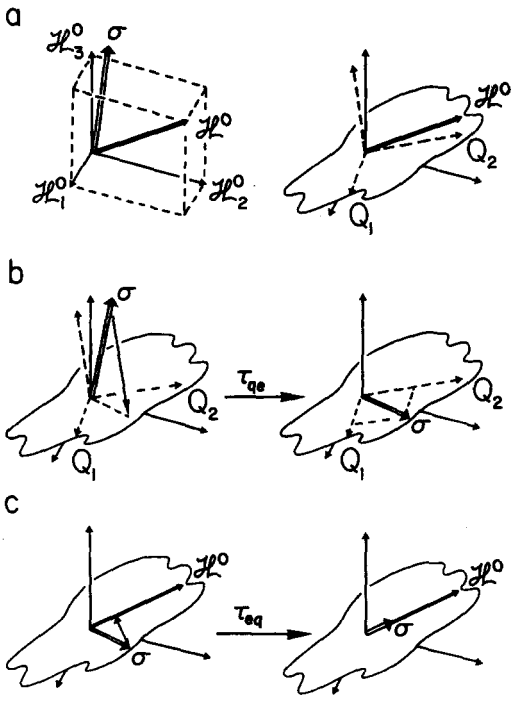

FIG. 3. Spin thermodynamics in the case of three thermodynamic reservoirs, $\mathcal{H}_1^0$, $\mathcal{H}_2^0$ and $\mathcal{H}_3^0$, which are represented in (a) as three orthogonal vectors with a sum vector $\mathcal{H}^0$. If internal thermal equilibrium is already established individually within each reservoir, the density operator σ may be represented as a three-dimensional vector in the $\{\mathcal{H}_1^0, \mathcal{H}_2^0, \mathcal{H}_3^0\}$ space. Other important vectors in the space are the two orthogonal quasi-invariants Q_1 and Q_2 which define a plane including $\mathcal{H}^0$. (b) Over a time τ_{eq}, a quasi-equilibrium state may be established which is represented as a projection of σ onto the $\{Q_1, Q_2\}$ plane. This is a metastable state of nonuniform spin temperature. (c) Over a sufficiently long time τ_{eq}, full thermal equilibrium may eventually be established which may be represented as a further projection of σ onto $\mathcal{H}^0$. In many circumstances this last step may be kinetically too slow to be observed and it is $\sigma(\tau_{\text{eq}})$ which is the experimentally relevant final state.

It is instructive to consider a pictorial representation of the quasi-equilibrium state (Fig. 3). Consider a system with three thermodynamic reservoirs, $\mathcal{H}_1^0$, $\mathcal{H}_2^0$, and $\mathcal{H}_3^0$, which are represented as three orthogonal vectors in Fig. 3(a). An arbitrary initial density operator would have to be represented as a vector of dimension greater than 3, providing graphical difficulties, so we accordingly proceed immediately to the state of internal thermal equilibrium within each reservoir, $\sigma(\tau_{\text{int}})$, Eq. (11). This density operator may be represented as a three-dimensional vector in the space spanned by $\{\mathcal{H}_1^0, \mathcal{H}_2^0, \mathcal{H}_3^0\}$ [Fig. 3(a)]. The establishment of quasi-equilibrium may be represented as the projection of the vector $\sigma(\tau_{\text{int}})$ onto a two-dimensional plane defined by the two orthogonal quasi-invariants Q_1 and Q_2 [Fig. 3(b)]. This plane contains the vector corresponding to the total Hamiltonian $\mathcal{H}^0 = \mathcal{H}_1^0 + \mathcal{H}_2^0 + \mathcal{H}_3^0$, and full thermal equilibration would consist of a further projection of the density operator onto this vector [Fig. 3(c)]. Again the successive projections of the density operator, first onto three-dimensional space (internal thermal equilibration of the three reservoirs), then onto a two-dimensional plane (establishment of quasi-equilibrium) and finally, if time allows, onto a one-dimensional vector (complete thermal equilibration) represent states of successively higher entropy. However the last

of these processes may be kinetically too slow to be observable leaving the quasi-equilibrium as the relevant state for the experimentally important time regime.

2. Thermodynamics of heteronuclear cross polarization

Referring to the specific case of cross polarization, we assume for now that there are three relevant reservoirs, $\mathcal{H}_I^T$, $\mathcal{H}_S^T$, and $\mathcal{H}_{II}^{T'}$, communicating by means of the heteronuclear coupling $V = \mathcal{H}_{IS}^T$. (The nonsecular coupling terms $\mathcal{H}_{II}^{T''}$ are ignored.) We note in passing that this division of the Hamiltonian is somewhat dangerous, since the heteronuclear couplings are of the same magnitude as the homonuclear couplings, so it may be invalid to assume that the reservoirs maintain internal thermal equilibrium rapidly compared to the rate of thermal contact between them: Nevertheless we continue with this assumption for the present. Near the Hartmann–Hahn condition, $\omega_{1S} \simeq \omega_{1I}$, it is possible to assume that exchange of order between $\mathcal{H}_I^T$ and $\mathcal{H}_S^T$ takes place by spin-pair flips, in which one I spin reverses its polarization in the rf field for every S spin, under the influence of the terms I^+S^- and I^-S^+ contained in the perturbation $V = \mathcal{H}_{IS}^T$. Near Hartmann–Hahn match, spin-pair flip processes produce only a small change in energy which is readily absorbed by the dipolar interactions. Since the operator $\Sigma_k I_{kz} + S_z$ commutes with I^+S^-, I^-S^+, and the other major Hamiltonian terms $\mathcal{H}_I^T$, $\mathcal{H}_S^T$, and $\mathcal{H}_{II}^{T'}$, it is plausible to associate a quasi-invariant operator Q_1 with it. The expectation value $\langle \Sigma_k I_{kz} + S_z \rangle$ then represents the total number of spins with magnetic quantum number $+1/2$ minus the number of spins with magnetic quantum number $-1/2$, a quantity (the *total angular momentum*) clearly conserved by spin-pair flips. Accordingly, the quasi-invariant operator Q_1 may be assigned

$$Q_1 = q_1 \left(\sum_k I_{kz} + S_z \right), \tag{15}$$

where the normalization factor

$$q_1 = \frac{\left(\mathcal{H}^0 \middle| \sum_k I_{kz} + S_z \right)}{\left(\sum_k I_{kz} + S_z \middle| \sum_k I_{kz} + S_z \right)} = \frac{N\omega_{1I} + \omega_{1S}}{N+1} \tag{16}$$

has been included for consistency with Eqs. (13). Here N is the number of abundant spins I communicating with a particular rare spin S on an experimental time scale. $\langle Q_1 \rangle$ then is the total Zeeman energy of all spins.

Note that under different experimental conditions different choices for this quasi-invariant may have to be made: For example, if $\omega_{1S} \simeq -\omega_{1I}$, an operator

$$Q_1' = \frac{N\omega_{1I} - \omega_{1S}}{N+1} \left(\sum_k I_{kz} - S_z \right)$$

is more appropriate. If $\omega_{1S} \simeq 2\omega_{1I}$, so that thermal equilibration takes place predominantly by three-spin flips, with one S spin flipping for every two I spins,

$$Q_1'' = \frac{N\omega_{1I} + 2\omega_{1S}}{N+4} \left(\sum_k I_{kz} + 2S_z \right)$$

would be the proper operator.[19–22]

We assume for now that Q_1 [Eq. (15)] is the only quasi-invariant of the system apart from the total energy (we will have to modify this assumption in the case of resolved couplings, see below). A quasi-invariant Q_2 is then formed by subtracting Q_1 from $\mathcal{H}^0$:

$$Q_2 = \mathcal{H}^0 - Q_1.$$

Providing Q_1 was properly normalized according to Eqs. (13) and (16), Q_2 is then orthogonal to Q_1. Q_2 may be evaluated in this case to be

$$Q_2 = \frac{\Delta\omega}{N+1} \left\{ NS_z - \sum_k I_{kz} \right\} + \mathcal{H}_{II}^{T'}, \tag{17}$$

where

$$\Delta\omega = \omega_{1S} - \omega_{1I}.$$

Note that the term Q_1 has distinct equally spaced eigenvalues, while for small mismatches $\Delta\omega \sim d_{jk}$, Q_2 has a dense quasicontinuous spectrum The quasi-equilibrium density operator is then calculated, assuming $N \gg 1$, to be

$$\begin{aligned} \sigma^T(\tau_{qe}) &\simeq Q_1 \frac{(\sigma^T(0)|Q_1)}{(Q_1|Q_1)} + Q_2 \frac{(\sigma^T(0)|Q_2)}{(Q_2|Q_2)} \\ &= \alpha_{0I} \left\{ S_z \frac{\lambda^2}{\lambda^2 + \Delta\omega^2} + \sum_k I_{kz} + \mathcal{H}_{II}^{T'} \frac{-\Delta\omega}{\lambda^2 + \Delta\omega^2} \right\}, \end{aligned} \tag{18}$$

with the cross-polarization width λ given by

$$\lambda^2 = \frac{(\mathcal{H}_{II}^{T'}|\mathcal{H}_{II}^{T'})}{(I_{kz}|I_{kz})} = \tfrac{1}{4} N M_2^I, \tag{19}$$

where M_2^I is the second moment of the I spin resonance line.[33]

Equation (18) predicts that the achievable S spin polarization is maximum on match, and falls off for both higher and lower rf field strengths ω_{1S} as a Lorentzian function of half-width at half-height $\lambda = \frac{1}{2}(N M_2^I)^{1/2}$. The Lorentzian dependence with a maximum on-match is qualitatively in accordance with experiment. It is also true that solids with large II couplings tend to have broad Hartmann–Hahn conditions, and that in substances where internal motions partially average out dipolar couplings, such as adamantane and hexamethylbenzene, the Hartmann–Hahn condition is narrow. However, quantitative agreement requires a proper choice for N, the number of I spins participating in cross polarization with a single S spin on an experimental time scale. It is tempting to assign to this number the ratio of the abundances of the two spin species in the crystal, about 150 for ^{1}H–^{13}C cross polarization. However, this yields too large a cross-polarization width λ, and the assumption that all spins in the crystal participate in the cross-polarization process also contradicts observations that lines originating from different ^{13}C sites in the same crystal may have different cross-polarization widths. It is perhaps best to leave N as a parameter which takes a value of the order of 10 and depends on the cross-polarization time, and to expect only qualitative agreement with experiment. Thus the theory presented here suggests that mismatched cross polarization of an S spin affects strongly dipolar II energies in the close vicinity of the S spin, but these energetic effects diffuse only slowly to I spins further removed from the cross-polarization site. A more

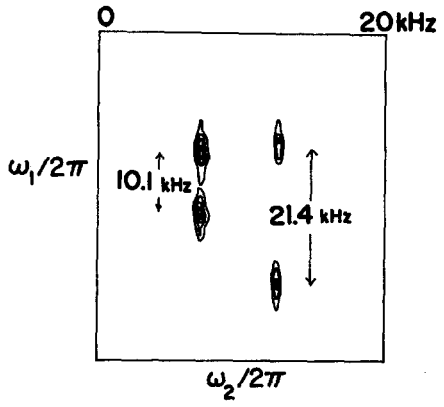

FIG. 4. Two-dimensional ^{13}C separated local field spectrum (Ref. 30) of a single crystal of ferrocene of unknown orientation. The two lines along the ω_2 axis arise from two nonequivalent crystal sites. Each of these shows a well-resolved splitting in the ω_1 dimension arising from dipolar coupling to the neighboring proton. All results shown below refer to the right-hand line which has $b_1/2\pi = 10.7$ kHz.

complete description might take into account spin-diffusion effects by a time-dependent broadening of the cross-polarization condition.

III. CROSS POLARIZATION IN SYSTEMS WITH RESOLVED HETERONUCLEAR INTERACTIONS

In many organic solids with short covalent bonds between ^{13}C and ^{1}H nuclei the ^{13}C "local field' is often dominated by a small number of short-range heteronuclear dipolar interactions. This is illustrated in Fig. 4 which is a two-dimensional "separated local field" spectrum of ferrocene, using the pulse sequence of Ref. 31 (without homonuclear decoupling during the evolution period). Chemical shifts are responsible for the spread along ω_2 while shifts and dipolar couplings are active along ω_1. The two nonequivalent ^{13}C sites display well resolved couplings to their directly bonded protons.

This resolved coupling structure has a strong influence on both the kinetics of cross polarization and the quasi-equilibrium position which is reached. The cross-polarized magnetization evolves in a damped oscillatory fashion,[27] especially near match, as is shown for one line of ferrocene in Fig. 5(b). Also the energetic effects of the strong heteronuclear couplings cannot be ignored, as was done in Sec. II, where the role of the heteronuclear couplings was assumed purely kinetic. The quasi-invariants must therefore be chosen taking into account the energetic and entropic influences of the resolved couplings. In the case of an S spin with a strong coupling to spin I_1, both spins being coupled more modestly to the remaining spins I_k $(k>1)$, the system is treated satisfactorily as the tightly coupled spin pair I_1S immersed in a bath consisting of the remaining protons.[27] We describe the dynamics in this case in two stages. First we treat the spin pair alone, paying particular attention to transient oscillations.[27] Then we allow the spin pair to come into thermodynamic contact with the remaining spins and discuss the quasi-equilibrium which is reached.

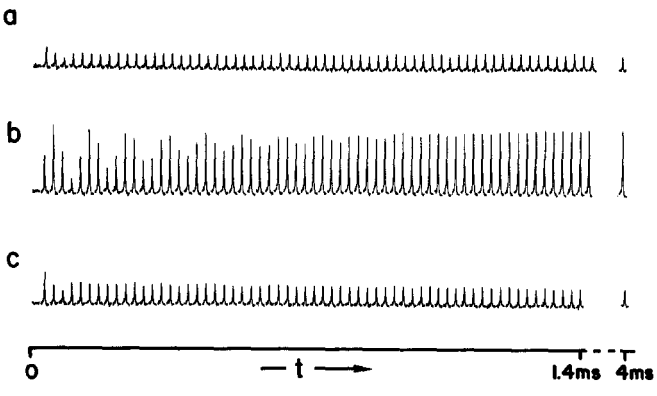

FIG. 5. The evolution of S magnetization $\langle S_x \rangle$ as a function of cross-polarization time t during a Hartmann–Hahn experiment for three different S spin rf field strengths, $\omega_{1S}/2\pi \simeq$ (a) 40 kHz, (b) 51 kHz, (c) 71.3 kHz. The I spin rf field was held constant at $\omega_{1I}/2\pi \simeq 54$ kHz. The transient oscillations described by Müller *et al.* (Ref. 27) are prominent near Hartmann–Hahn match (b). The described polarization of the S spins in (a) and (c) is clearly not a result of competing cross-polarization and spin-lattice relaxation, as is usually claimed, because the signal remains constant over a considerable period of time. It must be explained instead by the establishment of a quasi-equilibrium state.

A. The isolated spin pair

The Hamiltonian of the spin pair I_1S in the tilted frame is given by

$$\mathscr{H}^T_{\text{pair}} = \omega_{1I} I_{1z} + \omega_{1S} S_z + b_1 2 I_{1y} S_y. \tag{20}$$

It may be separated into two commuting parts:

$$\mathscr{H}^T_{\text{pair}} = \mathscr{H}^T_{\Sigma} + \mathscr{H}^T_{\Delta}, \tag{21}$$

with

$$\mathscr{H}^T_{\Sigma} = \omega_e^{\Sigma} I_e^{\Sigma}, \quad \mathscr{H}^T_{\Delta} = \omega_e^{\Delta} I_e^{\Delta},$$
$$\omega_e^{\Sigma} = [(\omega_{1S} + \omega_{1I})^2 + (b_1)^2]^{1/2},$$
$$\omega_e^{\Delta} = [(\omega_{1S} - \omega_{1I})^2 + (b_1)^2]^{1/2},$$
$$I_e^{\Sigma} = I_z^{\Sigma} \cos\theta^{\Sigma} + I_x^{\Sigma} \sin\theta^{\Sigma},$$
$$I_e^{\Delta} = I_z^{\Delta} \cos\theta^{\Delta} + I_x^{\Delta} \sin\theta^{\Delta},$$
$$I_z^{\Sigma} = \tfrac{1}{2}(I_{1z} + S_z), \quad I_z^{\Delta} = \tfrac{1}{2}(I_{1z} - S_z),$$
$$I_x^{\Sigma} = \tfrac{1}{2}(I_1^{+} S^{+} + I_1^{-} S^{-}) = \tfrac{1}{2}(2 I_{1x} S_x - 2 I_{1y} S_y),$$
$$I_x^{\Delta} = \tfrac{1}{2}(I_1^{+} S^{-} + I_1^{-} S^{+}) = \tfrac{1}{2}(2 I_{1x} S_x + 2 I_{1y} S_y),$$

and

$$\tan\theta^{\Sigma} = b_1/(\omega_{1I} + \omega_{1S});$$
$$\tan\theta^{\Delta} = b_1/(\omega_{1I} - \omega_{1S}) = -b_1/\Delta\omega. \tag{22}$$

The eigenvalues of $\mathscr{H}^T_{\text{pair}}$ are $\pm\frac{1}{2}\omega_e^{\Sigma}$ and $\pm\frac{1}{2}\omega_e^{\Delta}$ and are plotted against ω_{1S} in Fig. 6. The spin pair may be treated as two independent two-level systems, involving the inner and outer pair of energy levels and representing the zero and double quantum frame, respectively.

The equation of motion with the initial density operator

$$\sigma^T(0)_{\text{pair}} = \alpha_{0I} I_{1z} = \alpha_{0I}(I_z^{\Sigma} + I_z^{\Delta})$$

may be solved exactly:

$$\sigma^T(t)_{\text{pair}} = \sigma^T_{\Sigma}(t) + \sigma^T_{\Delta}(t), \tag{23}$$
$$\sigma^T_{\Sigma}(t) = \alpha_{0I}\{I_e^{\Sigma} \cos\theta^{\Sigma} + (I_z^{\Sigma} \sin\theta^{\Sigma} - I_x^{\Sigma} \cos\theta^{\Sigma}) \times \sin\theta^{\Sigma} \cos\omega_e^{\Sigma} t - I_y \sin\theta^{\Sigma} \sin\omega_e^{\Sigma} t\}, \tag{24}$$
$$\sigma^T_{\Delta}(t) = \alpha_{0I}\{I_e^{\Delta} \cos\theta^{\Delta} + (I_z^{\Delta} \sin\theta^{\Delta} - I_x^{\Delta} \cos\theta^{\Delta})$$

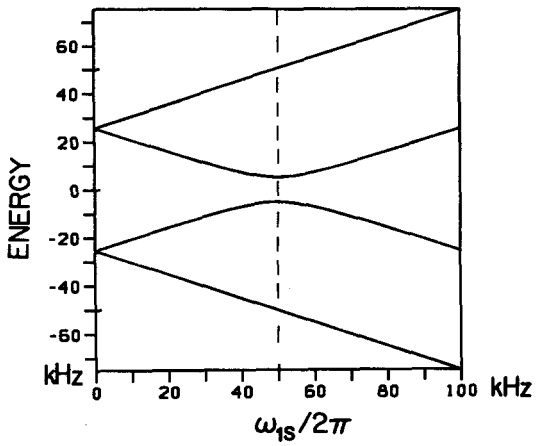

FIG. 6. The eigenvalues of $\mathscr{H}^T_{\text{pair}}$ [Eq. (20)] plotted against $\omega_{1S}/2\pi$ for $\omega_{1I}/2\pi = 50$ kHz and $b_1/2\pi = 10.7$ kHz. Near Hartmann–Hahn match (dashed line) the two central levels assume their minimum separation b_1 while the two outer levels have a separation close to $2\omega_{1I}/2\pi$.

$$\times \sin\theta^{\Delta}\cos\omega_e^{\Delta}t - I_y^{\Delta}\sin\theta^{\Delta}\sin\omega_e^{\Delta}t\}, \tag{25}$$

where the y components of the double and zero quantum operators are given by

$$I_y^{\Sigma} = \frac{1}{2i}(I_1^{+}S^{+} - I_1^{-}S^{-}) = \frac{1}{2}(2I_{1y}S_x + 2I_{1x}S_y)$$

and

$$I_y^{\Delta} = \frac{1}{2i}(I_1^{+}S^{-} - I_1^{-}S^{+}) = \frac{1}{2}(2I_{1y}S_x - 2I_{1x}S_y). \tag{26}$$

For strong rf fields, $|\omega_{1I} + \omega_{1S}| \gg b_1$, we may set $\cos\theta^{\Sigma} \simeq 1$ and $\sin\theta^{\Sigma} \simeq 0$ and Eq. (24) becomes

$$\sigma_{\Sigma}^T(t) \simeq \alpha_{0I} I_z^{\Sigma}. \tag{27}$$

The oscillations in Eq. (25) [visible in Fig. 5(b)] are those oberved by Müller *et al.*,[27] and may be used to derive the size of the heteronuclear coupling.[29] They arise because the density operator is prepared in a state off-diagonal with respect to the difference Hamiltonian $\mathscr{H}^T_{\Delta}$ of Eq. (21). The situation is depicted in Fig. 7, which shows the separate reference frames for $\mathscr{H}^T_{\Sigma}$ and $\mathscr{H}^T_{\Delta}$, the effective fields in these frames, and the oscillatory decay of the two independent components σ^T_{Σ} and σ^T_{Δ} of the density operator. In practice the oscillations die out fairly rapidly because of interactions with other spins I_k, and because of rf inhomogeneity. This leaves the time-independent parts of Eq. (23),

$$\sigma^T_{\text{pair}}(t \gg 0) = \alpha_{0I}\{I_z^{\Sigma} + I_e^{\Delta}\cos\theta^{\Delta}\}$$

$$= \alpha_{0I}\left\{I_{1z}\left[1 - \frac{1}{2}\frac{b_1^2}{\Delta\omega^2 + b_1^2}\right] + S_z\frac{1}{2}\frac{b_1^2}{\Delta\omega^2 + b_1^2} + \frac{1}{2}(2I_{1y}S_y + 2I_{1x}S_x)\frac{-\Delta\omega b_1}{\Delta\omega^2 + b_1^2}\right\}. \tag{28}$$

These equations predict that on-match, half the initial polarization of the I spin is transferred to the S spin. Off-match, the transferred polarization falls off as a Lorentzian function of half-width at half-height b_1, and heteronuclear dipolar order within the pair, $\langle 2I_{1y}S_y + 2I_{1x}S_x\rangle$, is created with a dispersion-Lorentzian dependence on $\Delta\omega$.

These predictions are in qualitative agreement with the experimental observations of Figs. 8(a) and 9(a), which show the quasi-equilibrium values of $\langle S_z\rangle^T = \langle S_x\rangle$ and $\langle 2I_{1y}S_y\rangle^T = \langle 2I_{1y}S_y\rangle$ as a function of rf field ω_{1S}, deter-

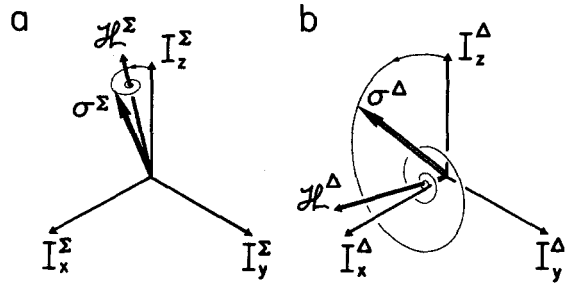

FIG. 7. Evolution of the density operator in time for an isolated spin pair during Hartmann–Hahn cross polarization close to match. The two parts of the density operator σ^{Δ} and σ^{Σ} precess independently around the Hamiltonians $\mathscr{H}^{\Delta}$ and $\mathscr{H}^{\Sigma}$. The precession is damped eventually by rf inhomogeneity, and in a realistic situation, by interactions with other spins. The large excursions of σ^{Δ} are responsible for the transient oscillations (Ref. 27).

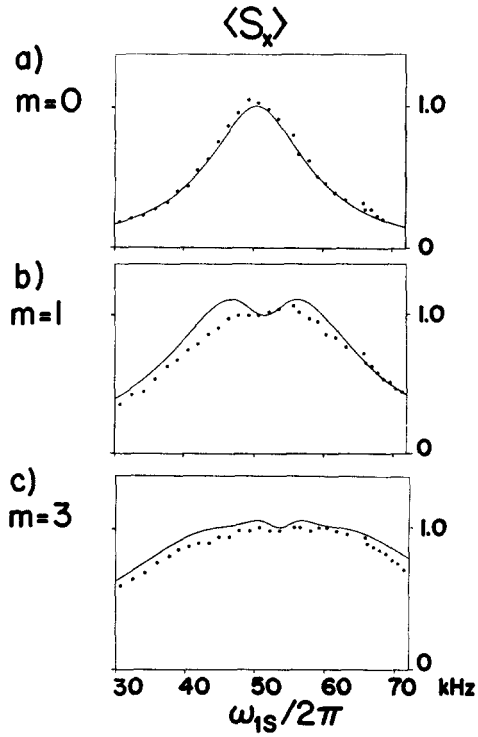

FIG. 8. Dependence of S spin polarization $\langle S_x\rangle$ for ferrocene on $\omega_{1S}/2\pi$ after cross polarization of duration 2 ms (a) without phase shifting, (b) with synchronous reversal of the phase of both I and S channels at time 1 ms, (c) with three synchronous phase reversals at time 500 μs, 1 ms, and 1.5 ms (see Fig. 11). The vertical scale is normalized such that normal cross polarization produces S spin polarization of unit magnitude on match. The theoretical curves are from Eq. (41), plotted in units of $\hbar\omega_{0I}/4kT$, with the dipolar coupling $b_1/2\pi = 10.7$ kHz (determined from Fig. 4) and $N = 10$, $\lambda/2\pi = 7.0$ kHz. These last two parameters were chosen for best fit to the data in (a). The rf field strength on the proton channel was slightly different in the three experiments due to instrumental variations, 50.4 kHz in (a), 51.5 kHz in (b), and 53.6 kHz in (c).

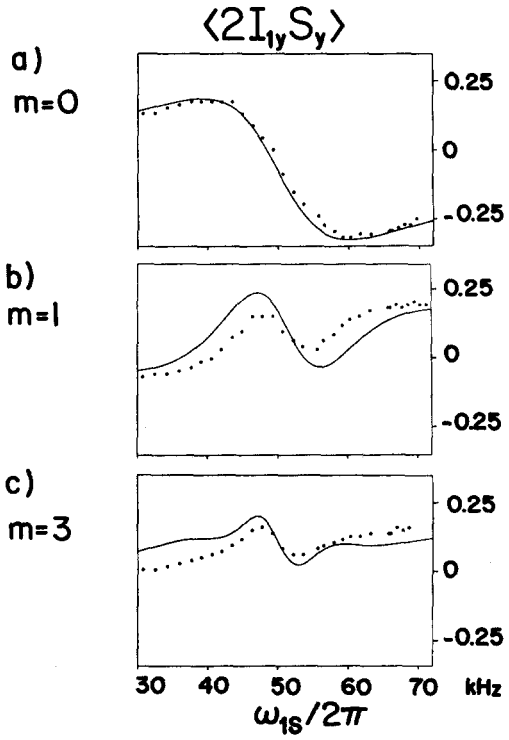

FIG. 9. As for Fig. 8, but with measurement of the expectation value $\langle 2I_{1y}S_y\rangle$ using the pulse sequence given in Fig. 13. The theoretical curves are for Eq. (41) with the same parameters as in Fig. 8.

mined by the method to be described in Sec. IV. ($\langle S_z\rangle^T$ refers to the tilted frame while $\langle S_x\rangle$ is evaluated in the laboratory frame.) The experimental results do verify the predicted absorption-Lorentzian form for $\langle S_x\rangle^T$ and the dispersion-Lorentzian form for $\langle 2I_{1y}S_y\rangle^T$. However, the following qualitative discrepancies are observed: (a) the relative magnitudes of $\langle S_z\rangle^T$ and $\langle 2I_{1y}S_y\rangle^T$ disagree with Eq. (28), $\langle S_z\rangle^T$ being about twice as large with respect to $\langle 2I_{1y}S_y\rangle^T$ as anticipated, (b) the dependence of $\langle 2I_{1y}S_y\rangle^T$ on ω_{1S} displays an approximately constant "offset" below zero superimposed on the dispersion-Lorentzian form, and (c) the width of the dispersion-Lorentzian part of $\langle 2I_{1y}S_y\rangle^T$ does correspond to the measured value of $b_1 = 10.7$ kHz, while the width of $\langle S_x\rangle^T$ is significantly smaller than this. All of these observations can be predicted by a refinement of the above model allowing relaxation of the assumption $|\omega_{1I} + \omega_{1S}| \gg |b_1|$, and including thermodynamic contact with the surrounding I spins, as is shown below.

B. Modified thermodynamic theory for resolved heteronuclear coupling

In a real situation the spin pair treated in the last section interacts with the surrounding protons and will tend to reach thermal equilibrium through spin diffusion. Full thermal equilibrium implies the establishment of population differences across the four spin pair transitions according to the prevailing spin temperature in the large proton reservoir, independent of the mode of preparation of the spin pair density operator. As is shown below, this is in fact in contradiction with experiment. To explain the observed behavior of the system, one must work with a more detailed theory, in

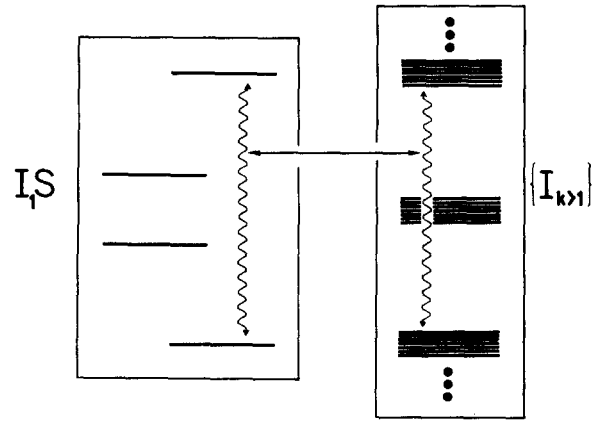

FIG. 10. Schematic drawing of the postulated thermodynamic processes occuring during cross polarization in ferrocene. The outer two levels of the I_1S spin pair have an energy separation roughly matching that between alternate energy level manifolds of the remaining protons I_k, and may exchange order by double-quantum spin diffusion. The central two levels of the I_1S pair are assumed to be thermally isolated.

which the sum term σ_Σ^T and the difference term σ_Δ^T reach equilibrium at markedly different rates.

The experimental results may be explained fairly closely if we assume that the term σ_Δ^T of the spin pair is thermally isolated from the reservoir of the remaining protons, while the sum term of the two-spin system comes into contact with the sum term of the proton bath.

A qualitative justification for this model is available from examination of the energy level diagram for the spin pair (Fig. 6). Close to match, the separation between the energy levels of the term $\mathcal{H}_\Delta^T$ is of the order of b_1. In the present system, this exceeds the homonuclear II couplings, so exchange of polarization between the term σ_Δ^T of the spin pair and the proton reservoir might be expected to be slow. On the other hand, the separation between the energy levels of $\mathcal{H}_\Sigma^T$ is close to $2\omega_{1I}$, which is the separation between alternate manifolds of the term $\mathcal{H}_I^T$. Hence thermal contact between these terms may be achieved by double-quantum spin diffusion (a transition between the two levels of $\mathcal{H}_\Sigma^T$ accompanied by a synchronous flip of two extraneous protons). Such double quantum spin-diffusion processes have been predicted and observed before.[26,34–41] The processes relevant for this model are shown schematically in Fig. 10.

We therefore postulate a quasi-invariant Q_1 whose expectation value will be conserved under the proposed double quantum thermal contact between the I spins and the two-level system $\mathcal{H}_\Sigma^T$. This will be the case if the quasi-invariant is proportional to $2I_e^\Sigma + \Sigma_{k>1} I_{kz}$ so we write

$$Q_1 = \frac{1}{N+2}(\omega_e^\Sigma + N\omega_{1I})\left(2I_e^\Sigma + \sum_{k=2}^{N+1} I_{kz}\right), \qquad (29)$$

where N is the number of I spins assumed to be in communication with the spin pair I_1S on an experimental time scale. The factor in Eq. (29) was chosen as in Eq. (16). Taking the perturbations V as

$$V = \mathcal{H}_{II}^{T''} + \sum_{k=2}^{N+1} b_k 2I_{kx}S_x,$$

and assuming thermal isolation of $\mathcal{H}_\Delta^T$, the remaining quasi-

invariants can be derived to be [through orthogonalization, see Eq. (16)]

$$Q_2 = \frac{1}{N+2}(\omega_e^{\Sigma} - 2\omega_{1I})\left(NI_e^{\Sigma} - \sum_{k=2}^{N+1} I_{kz}\right) + \mathscr{H}_{II}^{T'},$$

$$Q_3 = -\omega_e^{\Delta} I_e^{\Delta}. \tag{30}$$

Assuming now strong rf fields, $|\omega_{1S} + \omega_{1I}| \gg |b_1|$, and making the approximation $\omega_e^{\Sigma} \simeq \omega_{1S} + \omega_{1I}$, the quasi-equilibrium density operator $\sigma^T(\tau_{eq})$ may be derived:

$$\sigma^T(\tau_{qe}) = \alpha_{0I} \sum_{q=1}^{3} a_q Q_q, \tag{31}$$

where the coefficients a_q are evaluated as

$$\alpha_{0I} a_q = \frac{(\sigma^T(0)|Q_q)}{(Q_q|Q_q)},$$

$$a_1 = \frac{N+1}{\omega_{1S} + (N+1)\omega_{1I}},$$

$$a_2 = -\frac{1}{\Delta\omega}\cos^2\theta^{\lambda}, \tag{32}$$

$$a_3 = -\frac{1}{\omega_e^{\Delta}}\cos\theta^{\Delta},$$

where

$$\tan\theta^{\lambda} = -\frac{\lambda}{\Delta\omega}\sqrt{\frac{2(N+2)}{N}} \tag{33}$$

and λ has the significance of Eq. (19). The equations give the following quasi-equilibrium values of $\langle S_x\rangle$ and $\langle 2I_{1y}S_y\rangle$:

$$\langle S_x\rangle = \langle S_z\rangle^T = \frac{\hbar\omega_{0I}}{4kT}\frac{1}{2(N+2)}\{N\sin^2\theta^{\lambda} + (N+2)\sin^2\theta^{\Delta}\}, \tag{34}$$

$$\langle 2I_{1y}S_y\rangle = \langle 2I_{1y}S_y\rangle^T = \frac{\hbar\omega_{0I}}{4kT}\frac{1}{2}\left\{-\sin\theta^{\Sigma}\left(1 + \frac{N}{N+2}\sin^2\theta^{\lambda}\right) + \sin\theta^{\Delta}\cos\theta^{\Delta}\right\} \tag{35}$$

using

$$\alpha_{0I}\,\mathrm{Tr}\{S_x^2\} = \hbar\omega_{0I}/4kT.$$

These equations give an excellent fit to the experimental dependencies of $\langle S_x\rangle$ and $\langle 2I_{1y}S_y\rangle$ on ω_{1S} by assuming $N \sim 10$ and $\lambda/2\pi \sim 4.5$ kHz, and using the measured value $b_1/2\pi = 10.7$ kHz, as is demonstrated in Figs. 8(a) and 9(a). For $\langle S_x\rangle$ the functional form of Eq. (34) is the sum of two Lorentzians with almost equal intensities but unequal widths, one arising from σ_{Δ}^T and one from σ_{Σ}^T. The latter component is due to the postulated double quantum spin-diffusion process. In terms of quasi-invariants this process corresponds to an equilibration between the Zeeman part of Q_2 with heat capacity $\Delta\omega^2\{N/[2(N+2)]\}$ and the dipolar part $\mathscr{H}_{II}^{T'}$ with heat capacity λ^2. For $\langle 2I_{1y}S_y\rangle$ the form is a dispersion-Lorentzian of width b_1 superimposed on a negative term smaller by a factor of the order $\theta^{\Sigma} \sim b_1/(\omega_{1I} + \omega_{1S})$. This small term is responsible for the "offset" apparent in Fig. 9(a) and decreases approximately linearly with ω_{1S}, except for a Lorentzian "bump" around the match condition, although these details are barely visible in the theoretical curves. The good agreement between theory and experiment seems to suggest that the postulated quasi invariants of Eqs. (29) and (30) are a good approximation to reality.

We have also determined $\langle 2I_{1z}S_z\rangle = \langle 2I_{1x}S_x\rangle^T$ experimentally and shown that the results fit well the theoretical curve

$$\langle 2I_{1z}S_z\rangle = \langle 2I_{1x}S_x\rangle^T = \frac{\hbar\omega_{0I}}{4kT}\frac{1}{2}\left\{\sin\theta^{\Sigma}\left(1 + \frac{N}{N+2}\sin^2\theta^{\lambda}\right) + \sin\theta^{\Delta}\cos\theta^{\Delta}\right\}. \tag{36}$$

The results resemble Fig. 9(a) but with a positive rather than negative offset to the dispersion-like dependence.

This model of a spin pair in thermodynamic contact with the remaining protons through double quantum spin diffusion also helps to explain the time dependences of S spin magnetization shown in Fig. 5. The slowly damped transient oscillations are due to the σ_{Δ}^T part of the spin pair density operator, which communicates only weakly with the remaining protons. Superimposed on these oscillations is a rising exponential background which may be attributed to the equilibration of the σ_{Σ}^T part with the remaining protons via double quantum spin diffusion. On match, the time constant of the exponential process is determined as about 1 ms, which is qualitatively consistent with double quantum spin-diffusion process. However, simultaneous participation of a single quantum spin-diffusion process cannot be ruled out.

C. Mismatch-optimized *IS* transfer (MOIST)

The model described above predicts that in the case of mismatched cross polarization the remaining order in the difference reservoirs Q_2 and Q_3 limits the polarization of the S spin. Maximum enhancement is reached when the coefficients a_2 and a_3 vanish. In order to achieve complete cross polarization it is necessary to reduce these to zero. In this section it is shown that this can be approached by a modification of the experiment shown in Fig. 11. Instead of keeping the spin-locking fields of constant phase, simultaneous π phase shifts are introduced on both channels, separated by intervals long enough to allow the system to attain quasi-equilibrium before the next phase shift.

This has a strong effect on the efficiency of cross polarization away from match [Figs. 8(b) and 8(c)]. In the case

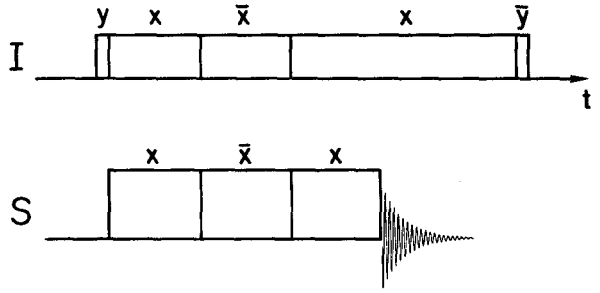

FIG. 11. Double irradiation scheme for the mismatch-optimized *IS* transfer (MOIST) experiment. This resembles normal Hartmann–Hahn cross polarization (Fig. 1) except for the synchronous phase reversals of the two spin-locking rf fields.

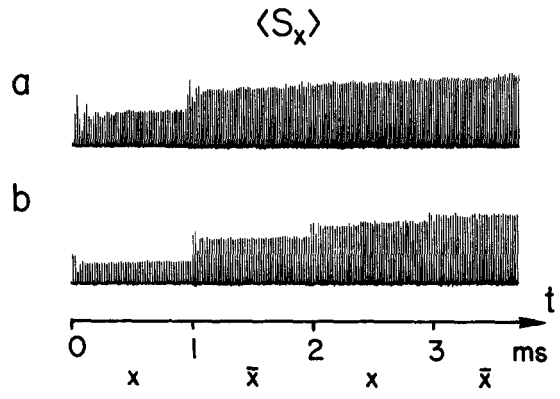

FIG. 12. Experimental time dependence of S spin polarization during a MOIST experiment. The phase of the two rf irradiation fields are reversed every 1 ms. The S spin polarization is monitored in steps of 20 μs. (a) $\omega_{1S}/2\pi = 38$ kHz, (b) $\omega_{1S}/2\pi = 31$ kHz. On each phase reversal, the system is displaced from equilibrium and after some period of transient oscillations settles into a new quasi-equilibrium with a larger S spin polarization.

shown, the introduction of three synchronous phase shifts increases the amount of polarization transferred by a factor of about two for mismatch $\Delta\omega/2\pi \sim 10$ kHz. The effect of the phase shifts is also shown in Fig. 12, in which the S spin polarization $\langle S_z \rangle^T$ is monitored in time through the experimental sequence under Hartmann–Hahn mismatched conditions. The application of a π phase shift in both irradiation channels is indicated on the time axis. Clearly, a new quasi-equilibrium is attained after each phase shift with progressively increased S spin polarization.

It is possible to explain the experimental results using the spin thermodynamic theory described in the previous section. The effect of the phase shift may be summarized as an inversion of all Zeeman terms in $\mathscr{H}^0$ and Q_q, while the dipolar terms remain invariant. The density operator of Eqs. (31) and (32) no longer commutes with the new Hamiltonian and therefore evolves towards a new equilibrium position. The quasi-invariants after m phase shifts may be written as

$$
\begin{aligned}
Q_1^{(m)} &= \frac{1}{N+2}\left[\omega_{1S} + (N+1)\omega_{1I}\right]\left\{2\left[I_z^\Sigma \cos\theta^\Sigma (-1)^m + I_x^\Sigma \sin\theta^\Sigma\right] + \sum_{k=2}^{N+1} I_{kz}(-1)^m\right\},\\
Q_2^{(m)} &= \frac{1}{N+2}\left(\omega_e^\Sigma - 2\omega_{1I}\right)\left\{N\left[I_z^\Sigma \cos\theta^\Sigma (-1)^m + I_x^\Sigma \sin\theta^\Sigma\right] - \sum_{k=2}^{N+1} I_{kz}(-1)^m\right\} + \mathscr{H}_{II}^{T'},\\
Q_3^{(m)} &= -\omega_e^\Delta\{I_z^\Delta \cos\theta^\Delta (-1)^m + I_x^\Delta \sin\theta^\Delta\}.
\end{aligned}
\tag{37}
$$

If the quasi-equilibrium density operator after phase shifts is written as

$$
\sigma^{(m)} = \alpha_{0I} \sum_{q=1}^{3} a_q^{(m)} Q_q^{(m)}. \tag{38}
$$

Then the coefficients $a_q^{(m+1)}$ are given by the recursions

$$
\begin{aligned}
a_1^{(m+1)} &= -a_1^{(m)},\\
a_2^{(m+1)} &= -a_2^{(m)} \cos(2\theta^\lambda),\\
a_3^{(m+1)} &= -a_3^{(m)} \cos(2\theta^\Delta).
\end{aligned}
\tag{39}
$$

Terms of order $(\theta^\Sigma)^2$ have been neglected. With the initial values $a_q^{(0)}$ given by Eq. (32) we find

$$
\begin{aligned}
a_1^{(m)} &= (-1)^m \frac{N+1}{\omega_{1S} + (N+1)\omega_{1I}},\\
a_2^{(m)} &= (-1)^m \left(-\frac{1}{\Delta\omega}\right) \cos^2\theta^\lambda \cos^m(2\theta^\lambda),\\
a_3^{(m)} &= (-1)^m \left(-\frac{1}{\omega_e^\Delta}\right) \cos\theta^\Delta \cos^m(2\theta^\Delta).
\end{aligned}
\tag{40}
$$

And for the expectation values of the experimental observables

$$
\begin{aligned}
\langle S_x \rangle^{(m)} &= \langle S_z \rangle^{T(m)}\\
&= \frac{\hbar\omega_{0I}}{4kT} \frac{1}{2(N+2)} \{N\left[1 - \cos^2\theta^\lambda \cos^m(2\theta^\lambda)\right]\\
&\quad + (N+2)\left[1 - \cos^2\theta^\Delta \cos^m(2\theta^\Delta)\right]\}\\
\langle 2I_{1y}S_y \rangle^{(m)} &= \langle 2I_{1y}S_y \rangle^{T(m)}\\
&= \frac{\hbar\omega_{0I}}{4kT}(-1)^m \frac{1}{2(N+2)}\\
&\quad \times\{-\theta^\Sigma[2N + 2 - N\cos^2\theta^\lambda \cos^m(2\theta^\lambda)]\\
&\quad + (N+2)\sin\theta^\Delta \cos\theta^\Delta \cos^m(2\theta^\Delta)\}.
\end{aligned}
\tag{41}
$$

The theoretical curves corresponding to these equations, using the same parameters as used to fit Figs. 8(a) and 9(a), are compared with the experimental results for $m = 1$ and 3 in Figs. 8(b) and 8(c) and 9(b) and 9(c). Agreement is not exact, but the equations do predict the right qualitative behavior, which is gratifying considering the complexity of the problem and the comparative simplicity of the theoretical model.

The remaining discrepancies between theory and exper-

iment, particularly in the forms for the dipolar order after a number of synchronous phase shifts, suggest that the assumption of the two central levels of the spin pair being thermally isolated is questionable. So far we have not been able to find forms for the quasi-invariants which take into account thermal leakage from the term Q_3. It may be that better agreement can be attained only by considering the kinetic approach to quasi-equilibrium.

IV. MEASUREMENT OF OBSERVABLES

The measurement of observables in solids such as ferrocene where large heteronuclear couplings are present is associated with particular problems. Methods will be described here which were used to obtain the experimental measurements $\langle S_z\rangle^T$ and $\langle 2I_{1y}S_y\rangle^T$ shown in Sec. III.

The tilted frame observables $\langle S_z\rangle^T$ and $\langle 2I_{1y}S_y\rangle^T$ are equal to the normal rotating frame observables $\langle S_x\rangle$ and $\langle 2I_{1y}S_y\rangle$. To a good approximation $\langle S_x\rangle$ may be measured directly as the intensity of the S spin signal in the presence of a strong decoupling rf field on the I spins, which narrows the resonance line and improves the sensitivity. $\langle 2I_{1y}S_y\rangle$ may be measured by applying a $(\pi/2)_x$ pulse on the I spins, allowing free evolution for a time $\tau=\pi/(4b_1)$, and then again measuring the I spin decoupled S signal intensity. However, if the attainable I spin decoupling field and the large heteronuclear coupling b_1 are of the same order of magnitude, it can no longer be assumed that the S spin signal gives an accurate measure of $\langle S_x\rangle$. Under these conditions, the decoupling irradiation may mix in some heteronuclear multiple-quantum contributions to the signal, as has recently been pointed out.[42]

The situation may be analyzed as follows. Consider the I_1S pair under strong irradiation of the I spins at a frequency halfway between the two unperturbed transitions of the I spin. The rotating frame Hamiltonian, assuming on-resonance S spins and neglecting distant I spins for simplicity, is given by

$$\mathscr{H}=b_1 2I_{1z}S_z+\omega_{1I}I_{1x} \tag{42}$$

which may be expressed in the form[43]

$$\mathscr{H}=\omega_e \exp(i\theta 2I_{1y}S_z)I_{1x}\exp(-i\theta 2I_{1y}S_z), \tag{43}$$

where

$$\tan\theta=b_1/\omega_{1I} \quad \text{and} \quad \omega_e=[\omega_{1I}^2+b_1^2]^{1/2}.$$

Suppose the density operator is prepared in the state $\sigma(0)$ and the S spin signal measured over a subsequent time t. Its value is

$$\langle S_x\rangle(t)=\mathrm{Tr}\{U(t)\sigma U(t)^{-1}S_x\}, \tag{44}$$

where

$$U(t)=\exp(i\theta 2I_{1y}S_z)\exp(i\omega_e tI_{1x})\exp(-i\theta 2I_{1y}S_z).$$

Equation (44) can be rearranged to give

$$\langle S_x\rangle(t)=\mathrm{Tr}\{\sigma U(t)^{-1}S_xU(t)\}, \tag{45}$$

and for small θ,

$$U(t)^{-1}S_xU(t)\simeq S_x+\theta 2I_{1y}S_y(1-\cos\omega_e t)+\theta 2I_{1z}S_z\sin\omega_e t. \tag{46}$$

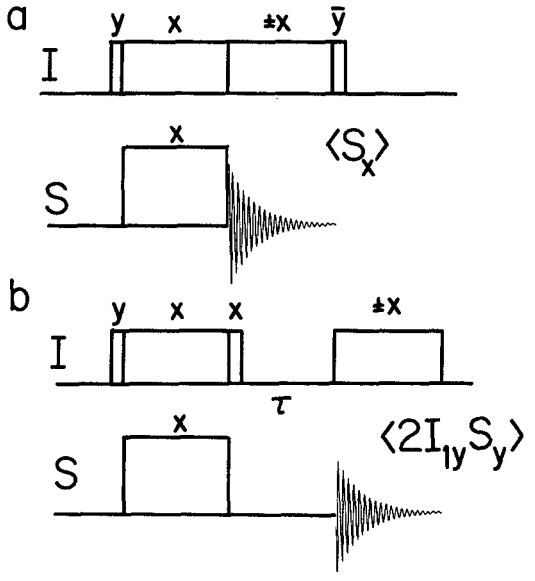

FIG. 13. Experimental schemes for measuring (a) $\langle S_x\rangle$ and (b) $\langle 2I_{1y}S_y\rangle$. Results are added from two different experiments with opposite decoupler phase to remove signals induced by heteronuclear multiple quantum coherence (see the text). In (b) an additional 90°_x pulse on the I spins followed by a delay of duration $\tau=\pi/(4b_1)$ is included.

Neglecting fast oscillating terms, which only produce weak high-frequency sidebands in the transformed signal, we find

$$\langle S_x\rangle(t)\simeq\mathrm{Tr}\{\sigma(0)S_x\}+\theta\,\mathrm{Tr}\{\sigma(0)2I_{1y}S_y\}, \tag{47}$$

showing that multiple quantum coherence represented by $2I_{1y}S_y$ directly induces an S spin signal in this case, although it is by a factor of $\theta\sim b_1/\omega_{1I}$ weaker than the conventional signal due to S spin magnetization. Nevertheless it can easily be distinguished because it is inverted if the phase of the I spin decoupler field is shifted by π. We have observed such effects, and found it necessary to eliminate unwanted multiple quantum signals by coadding two sets of data with opposite phases. This was particularly important in the case of mismatched cross polarization where terms $2I_{1y}S_y=(2I_{1y}S_y)^T$ are present in quasi-equilibrium [Eqs. (35) and (41)]. Figure 13 summarizes the pulse sequences used to obtain accurate measurements of $\langle S_x\rangle$ and $\langle 2I_{1y}S_y\rangle$.

V. CONCLUSIONS

This paper should make it clear that the process of Hartmann–Hahn cross polarization is more subtle and complicated than might be thought at first. The common description which disregards the thermodynamic influence of the dipolar couplings qualitatively disagrees with the experimental behavior. A proper account of the quantization of the I and S spin reserviors and the involvement of the dipolar couplings to absorb energy mismatches must be made. The theoretical apparatus described here seems to reach qualitative agreement with experiment as far as quasi-equilibrium observables are concerned. However there is a certain amount of arbitrariness in the construction of the quasi-invariants. In addition to the present thermodynamic treatment, a more thorough description of the time behavior would also be desirable.

A modification of the usual experiment was suggested

which involves repeated simultaneous π phase shifts of the two channels. It allows efficient cross polarization even under Hartmann–Hahn mismatch conditions. The technique is effective for static samples if a strong heteronuclear coupling exists which can contain the heteronuclear dipolar order. It might be worth considering in cases where power considerations or differential rf inhomogeneities for the two channels make it difficult to attain Hartmann–Hahn match.

ACKNOWLEDGMENTS

We would like to thank Professor J. Jeener for many enlightening discussions, P. Caravatti and G. Bodenhausen for instrumental help, and Miss I. Müller for patiently editing an illegible manuscript.

[1]S. R. Hartmann and E. L. Hahn, Phys. Rev. **128**, 2042 (1962).
[2]F. M. Lurie and C. P. Slichter, Phys. Rev. **133**, A1108 (1964).
[3]D. A. McArthur, E. L. Hahn, and R. E. Walstedt, Phys. Rev. **188**, 609 (1969).
[4]P. K. Grannell, P. Mansfield, and M. A. B. Whitaker, Phys. Rev. B **8**, 4149 (1973).
[5]A. Pines, M. G. Gibby, and J. S. Waugh, J. Chem. Phys. **59**, 569 (1973).
[6]C. P. Slichter, *Principles of Magnetic Resonance*, 2nd ed. (Springer, Berlin, 1980).
[7]M. Mehring, *High Resolution NMR Spectroscopy in Solids*, 2nd ed. (Springer, Berlin, 1983).
[8]E. O. Stejskal, J. Schaefer, and J. S. Waugh, J. Magn. Reson. **28**, 105 (1977).
[9]L. Müller, Chem. Phys. **61**, 235 (1981).
[10]S. Vega, T. W. Shattuck, and A. Pines, Phys. Rev. A **22**, 638 (1980).
[11]P. Brunner, M. Reinhold, and R. R. Ernst, J. Chem. Phys. **73**, 1086 (1980).
[12]S. Vega, Phys. Rev. A **23**, 3152 (1981).
[13]T. K. Pratum and M. P. Klein, J. Magn. Reson. **55**, 421 (1983).
[14]L. Müller and R. R. Ernst, Mol. Phys. **38**, 963 (1979).
[15]G. C. Chingas, A. N. Garroway, R. D. Bertrand, and W. B. Moniz, J. Chem. Phys. **74**, 127 (1981).
[16]D. E. Demco, J. Tegenfeldt, and J. S. Waugh, Phys. Rev. B **11**, 4133 (1975).
[17]B. N. Provotorov, Soviet Phys. JETP **15**, 611 (1962).
[18]J. Philippot, Phys. Rev. **133**, A471 (1964).
[19]J. Jeener, H. Eisendrath, and R. von Steenwinkel, Phys. Rev. **133**, A478 (1964).
[20]R. L. Kyhl and B. D. Nageswara-Rao, Phys. Rev. **158**, 284 (1967).
[21]J. Jeener, Adv. Magn. Reson. **3**, 205 (1968).
[22]M. Goldman, *Spin Temperature and Nuclear Magnetic Resonance in Solids* (Clarendon, Oxford, 1970), p. 160.
[23]M. A. B. Whitaker, Phys. Status Solidi B **79**, 673 (1977); **83**, 573 (1977); **84**, 149 (1977); **87**, 689 (1978).
[25]R. Grosescu, M. Velter-Stefanescu, and P. Draghicescu, Rev. Roum. Phys. **23**, 703 (1978).
[26]M. A. B. Whitaker, Phys. Status Solidi B **98**, 449 (1980).
[27]L. Müller, Anil Kumar, T. Baumann, and R. R. Ernst, Phys. Rev. Lett. **32**, 1402 (1974); L. Müller, Anil Kumar, T. Baumann, and R. R. Ernst, Proc. 18th Ampere Congress, Nottingham 1974, p. 557.
[28]W. P. Aue, E. Bartholdi, and R. R. Ernst, J. Chem. Phys. **64**, 2229 (1976).
[29]R. K. Hester, J. L. Ackerman, V. R. Cross, and J. S. Waugh, Phys. Rev. Lett. **34**, 993 (1975).
[30]R. K. Hester, J. L. Ackerman, B. L. Neff, and J. S. Waugh, Phys. Rev. Lett. **36**, 1081 (1976).
[31]E. F. Rybaczewski, B. L. Neff, and J. S. Waugh, J. Chem. Phys. **67**, 1231 (1977).
[32]J. Tegenfeldt and U. Haeberlen, J. Magn. Reson. **36**, 453 (1979).
[33]A. Abragam, *The Principles of Nuclear Magnetism* (Clarendon, Oxford, 1961).
[34]P. Mansfield and G. P. Cant, Phys. Lett. A **33**, 130 (1970).
[35]M. Kunitomo, J. Phys. Soc. Jpn. **30**, 1059 (1971).
[36]M. Kunitomo and T. Hashi, Phys. Lett. A **41**, 231 (1972).
[37]M. Kunitomo, H. Hatanaka, and T. Hashi, J. Phys. Soc. Jpn. **42**, 453 (1977).
[38]W. J. C. Grant, Phys. Rev. **134**, A1565 (1964).
[39]R. Eckman, A. Pines, R. Tycko, and D. P. Weitekamp, Chem. Phys. Lett. **99**, 35 (1983).
[40]C. Ye, R. Eckman, and A. Pines, J. Magn. Reson. **55**, 334 (1983).
[41]D. Suter and R. R. Ernst, Phys. Rev. B **32**, 5608 (1985).
[42]P. H. Bolton, J. Magn. Reson. **62**, 163 (1985).
[43]O.W. Sørensen, G. W. Eich, M. H. Levitt, G. Bodenhausen, and R. R. Ernst, Progr. NMR Spectrosc. **16**, 163 (1983).